Toxicology Reports 2 (2015) 1007–1013

Contents lists available at ScienceDirect

Toxicology Reports

journal homepage: www.elsevier.com/locate/toxrep

New CeO_2 nanoparticles-based topical formulations for the skin protection against organophosphates

Arnaud Zenerino[a], Tifenn Boutard[b,c], Cécile Bignon[a], Sonia Amigoni[a], Denis Josse[d], Thierry Devers[c], Frédéric Guittard[a,*]

[a] Université de Nice Sophia-Antipolis, Laboratoire de Physique de la Matière Condensée - UMR CNRS 7336, Groupe Surfaces et Interfaces, Parc Valrose, 06108 Nice Cedex 2, France
[b] ABC Texture, rue Isaac Newton, 35800 Dinard, France
[c] Centre de Recherche de la Matière Divisée (CRMD) – FRE 3520, IUT de Chartres, Université d'Orléans, 21, rue de Loigny la Bataille, 28000 Chartres, France
[d] Départemental d'Incendie et de Secours des Alpes-Maritimes, 140, Avenue de Lattre de Tassigny BP99, 06271 Villeneuve Loubet Cedex, France

ARTICLE INFO

Article history:
Received 13 May 2015
Received in revised form 29 June 2015
Accepted 5 July 2015
Available online 13 July 2015

Keywords:
Topical skin protection
Paraoxon
Cerium dioxide
Nanoparticles
Thickening polymers

ABSTRACT

To reinforce skin protection against organophosphates (OPs), the development of new topical skin protectants (TSP) has received a great interest. Nanoparticles like cerium dioxide (CeO_2) known to adsorb and neutralize OPs are interesting candidates for TSP. However, NPs are difficult to disperse into formulations and they are suspected of toxicological issues. Thus, we want to study: (1) the effect of the addition of CeO_2 NPs in formulations for the skin protection (2) the impact of the doping of CeO_2 NPs by calcium; (3) the effect of two methods of dispersion of CeO_2 NPs: an O/W emulsion or a suspension of a fluorinated thickening polymer (HASE-F) grafted with these NPs. As a screening approach we used silicone membranes as a skin equivalent and Franz diffusion cells for permeation tests. The addition of pure CeO_2 NPs in both formulations permits the penetration to decrease by a 3–4-fold factor. The O/W emulsion allows is the best approach to obtain a film-forming coating with a good reproducibility of the penetration results; whereas the grafting of NPs to a thickener is the best way to obtain an efficient homogenous suspension of CeO_2 NPs with a decreased of toxicological impact but the coating is less film-forming which slightly impacts the reproducibility of the penetration results.

1. Introduction

Human exposure to organophosphates (OPs) can occur in domestic, occupational and incidental contexts. [1–3]. They are used as pesticides (parathion, malathion, etc.) [4] and the most toxic of them are part of chemical warfare agents (CWA) (sarin, VX, etc.) [5]. They inhibit acetylcholinesterases (AChE) present in the central and peripheral nervous system. This results in an accumulation of the acetylcholine (ACh) neurotransmitter that causes paralysis, suffocation and death [5]. The main exposure routes to OPs are respiratory and dermal. Percutaneous penetration can occur for the most persistent of them such as the CWA VX and the pesticide parathion and its oxidized derivative paraoxon (POX) [6–8]. As a consequence, specific protective equipments (suits, face masks, gloves and boot covers) were developed to limit skin contact and absorption of these highly toxic chemicals [9]. However, they are not adapted to all situations and need to be perfectly adjusted [10]. To reinforce skin protection, topical skin protectants (TSP) or barrier creams (BC) mainly constituted of perfluorinated polymers and reactive compounds have received a great interest [11–16]. Nanoparticles (NPs) materials such as silica, titanium oxide or cerium oxide have been studied for their capacity to adsorb and neutralize toxic compounds including OPs [11,13,15,17–27]. In particular, cerium dioxide (CeO_2) NPs that are used in many fields (solar cells [28], as catalysts [29] and ultraviolet absorbents) [30–32] were demonstrated to hydrolyse phosphate ester bonds [33]. Moreover, it has been shown that the doping of CeO_2 NPs by calcium modify their structure and their physicochemical properties resulting in an increase of their UV filtration [32]. These modifications could also be interesting for our purpose. Then, the introduction of CeO_2 or calcium doped-CeO_2 (Ca^{2+}-CeO_2) NPs into emulsions could be a new way to improve the TSP efficacy against OPs [32,34].

Due to potential aggregation of NPs in emulsion, their skin permeation and potential toxicity [35–40], another innovative way is to graft them onto thickening polymers [41].

* Corresponding author.
E-mail address: guittard@unice.fr (F. Guittard).

http://dx.doi.org/10.1016/j.toxrep.2015.07.003

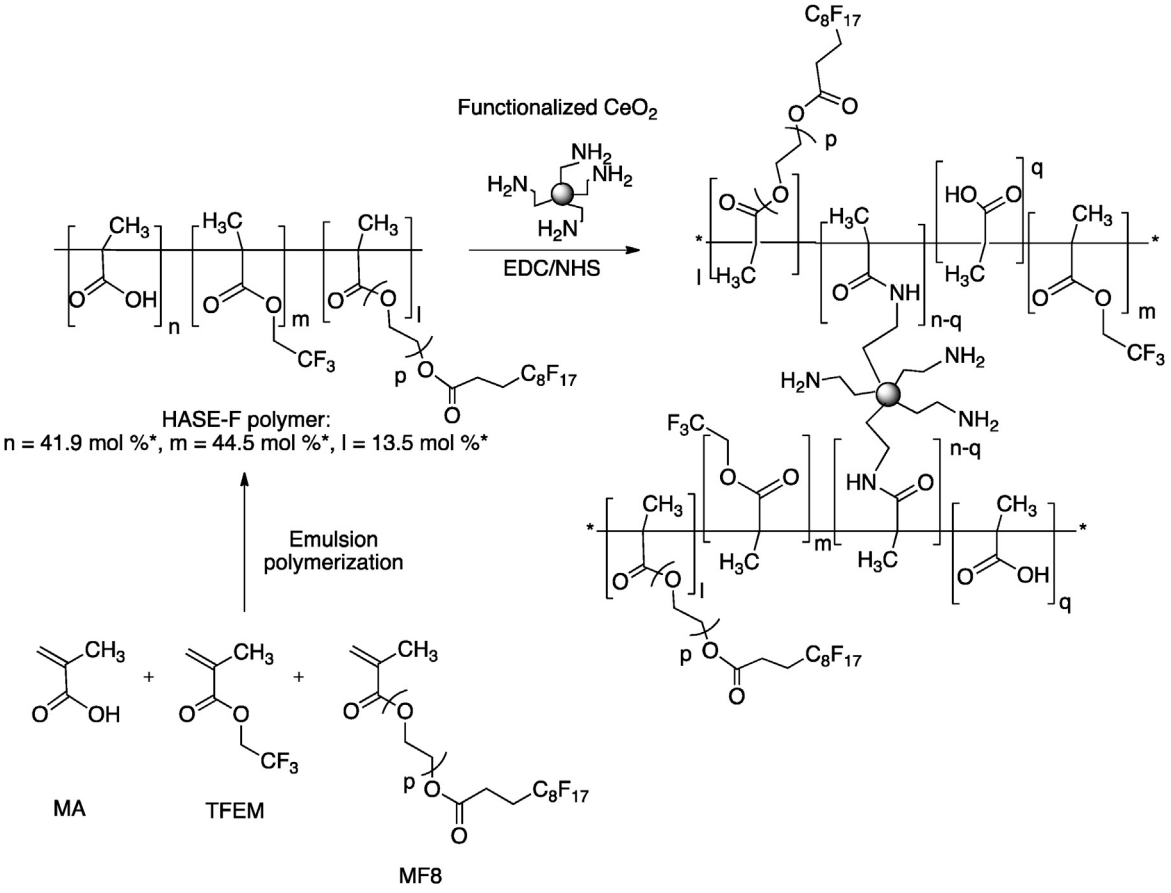

Fig. 1. Grafting of amine-functionalized CeO_2 NPs to the HASE-F polymer.

Thickeners are associative polymers such as hydrophobically modified alkali-soluble emulsion (HASE) that have the ability to form three-dimensional network gels in aqueous solution. The backbone of these copolymers is constituted of methacrylic acid (MA), ethyl acrylate (EA) and a small amount of associative macromonomer (M). The macromonomer contains a hydrophobic pendant group separated from the backbone by a polyethylene glycol (PEG) spacer chain. These thickening agents typically combine two properties: the solubility in alkaline solution due to the presence of carboxylic groups that ionise and provoke an increase of hydrodynamic volume, and the existence of Van der Walls interactions between the polymeric chains for an increase of the aqueous solution viscosity [42–44]. The substitution of hydrocarbon moieties into fluorinated ones in the copolymer leads to very low surface tension copolymers, and often improves the dispersibility of nanoparticles in water [42,43,45–48]. Our recent works demonstrated that the total replacement of ethyl groups in an HASE skeleton by trifluoroethyl groups (HASE-F polymer) leads to solutions with a thickening effect equivalent to the reference hydrocarbon HASE [49]. The covalent grafting of NPs on HASE polymers allows the creation of a nanoparticular network [41] which can (1) combine both protective/decontamination effects of fluorinated polymers and NPs and (2) decrease NPs impact on the environment [50].

In this work, our goals were: (1) to observe the impact of the doping of CeO_2 NPs by calcium for the skin protection against OPs; and (2) to determine the effect of two dispersion methods on the effectiveness of CeO_2 NPs. The efficacy of two CeO_2 NP-based topical formulations was evaluated: in the first one, CeO_2 NPs were dispersed in an O/W emulsion; in the second one, NPs were grafted onto a fluorinated HASE thickener polymer (HASE-F) (Fig. 1).

Millerioux *et al.* [6,7] showed that in vitro permeation tests using silicone membranes are suitable as first screen tests to select potentially effective TSP against toxic chemicals agents. Thus, efficacy test were performed with in vitro Franz-type glass diffusion cells using silicone membranes as a support matrix representing the skin. The toxic model OPs agent was paraoxon (POX) since it has similar physicochemical properties than some highly toxic OPs (VX, soman, etc.) [7] but it is much less toxic, making it safer to handle.

2. Experimental

2.1. Reagents and instrumentation

All reagents were obtained from Sigma–Aldrich. Microwave treatment of the samples was realized in a Multiwave 300 (Anton Paar). The crystalline structure was identified by X-ray diffraction (XRD) using the Cu Kα wavelength (λ = 0,1542 Å) of a X'Pert Pro X-ray diffractometer from PANanalytical. The specific surface area of the samples was measured by the Brunauer–Emmett–Teller (BET) method with a Nova 1000 high speed gas sorption analyser from Quantachrome. IR spectra were recorded on FTIR Spectrometer PARAGON 1000 from PerkinElmer by potassium bromide pellet method.

2.2. NPs synthesis and characterisation

Pure CeO_2 powders were synthesized by a microwave-hydrothermal method, previously published [39]. Briefly a 0.5 mol/L cerium nitrate solution $Ce(NH_4)_2(NO_3)_6$ was mixed with 2 mol/L sodium hydroxide solution at room temperature (~20 °C).

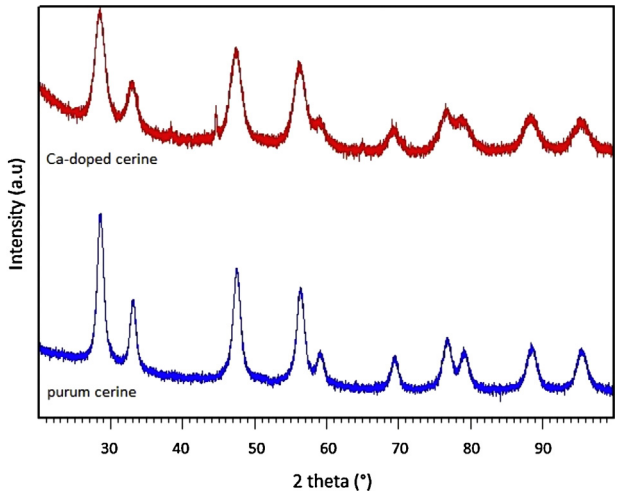

Fig. 2. XRD patterns of the pure (blue) and the doped CeO_2 (red) nanoparticles.

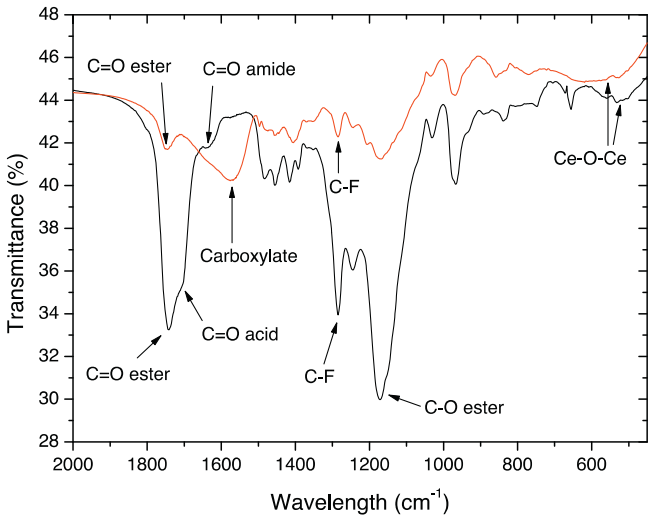

Fig. 3. FTIR spectrum of HASE-F/Ce in neutral (black curve) and basic middle (red curve).

The mixture was introduced in a silicon carbide crucible and treated in a microwave during 15 min at 90 °C and maximum pressure of 10 bars. The resulting precipitate was recovered by centrifugation, washed three times with deionized water and dried in air during 3 h. The obtained compound was then treated in air at 500 °C during 2 h. The calcium doped CeO_2 powders were synthesized by adding a $Ca(NO_3)_2{,}4H_2O$ solution to the initial solution in order to obtain the final doping at 15 mol.% of Ca^{2+}. This percentage was chosen to achieve the recommended dose of doping to observed a gain in the efficiency of UV protection (>10%) [32].

The XRD patterns of the pure and the doped CeO_2 nanoparticles show that they only contain the CeO_2 phase, which has a fluorite type cubic structure (JCPDS 34-394) (Fig. 2). Physicochemical properties are presented in Table 1. The CeO_2 lattice parameter increases with doping NPs, due to the Ca^{2+} effective ionic radius (1.12 Å), which is larger than that of Ce^{4+} (0.97 Å). The crystallite size was calculated by Sherrer's formula.

2.3. Dispersion of NPs in emulsions

Three O/W emulsions containing 5% of perfluorinated polymers (PTFE, Polymist F5a), 5% silicones (standard dimethicone) and 10% paraffin associated with or without cerium NPs were prepared: H21, H21CeO_2 and H21CeO_2–Ca^{2+}. Commonly, the rate of active ingredients is from 2% to 25% of the formula then we chose to use NP at 10%. H21 base did not contain NPs, H21CeO_2 contained 10% of pure CeO_2 NPs and H21CeO_2–Ca^{2+} contained 10% of Ca^{2+}-doped CeO_2 NPs.

2.4. Synthesis and characterization of CeO_2 grafted to HASE copolymer

2.4.1. Functionalization of NPs

2 g of CeO_2 NPs, obtained from Truffault *et al.* [32] (diameter: 8.3 nm, crystallite size: 9.3 nm and lattice parameter: 0.5410) were functionalized as described previously [41]. The amount of amino groups was determined by elemental analysis: 0.86 mmol/g.

IR (main vibrations): $\nu = 3420\,cm^{-1}$ (hydroxyl groups (—OH) of Ce—OH and water), 2925 cm^{-1} (alkyl groups of amino-silane (—CH_2)), 1630 cm^{-1} (hydroxyl groups of water (—OH)), 1500 cm^{-1} (N—H vibration of amine), 450–500 cm^{-1} (Ce—O—Ce vibration).

2.4.2. Grafting of NPs to the HASE copolymer

Functionalized CeO_2 NPs were grafted on fluorocarbon copolymer previously synthetized (HASE-F containing 13.5 mol.% of long fluorinated chain). The reaction was similar to that realized for silica NPs in a previous work [41] excepted that the equivalent ratio between —NH_2 and —COOH groups was 0.13 eq (2.6 mmol of —NH_2) for CeO_2 NPs instead of 0.3 eq (5.7 mmol of —NH_2). Fig. 3 represents FTIR spectra of HASE-F/Ce in neutral and basic aqueous solution. In basic medium, the carboxylic acid ionizes and the corresponding carbonyl band is shifted from 1704 cm^{-1} to 1570 cm^{-1} (strong asymmetrical stretching band) whereas the amide carbonyl band stays at 1638 cm^{-1} and the ester one at 1741 cm^{-1}. Moreover, in basic and neutral medium the fluorocarbon band, C—O ester band, and Ce—O—Ce band are at 1285 cm^{-1}, 1170 cm^{-1}, and 523 cm^{-1}, respectively. IR analysis showed the presence of residual free carboxylic acid functionalities that are necessary for the swelling of the resulting compound in water and the dispersion of nanoparticles in solution.

2.5. In vitro permeation studies

In vitro studies were conducted under a hood at room temperature (~20 °C).

2.5.1. Preparation of silicone membranes

A roll of silicone membrane of 400 ± 100 μm thickness was provided by Samco Silicone Products (Nuneaton, UK). On the day of experiment, it was cut into 9.42 cm^2-surface area disks that were then soaked in distilled water for 30 min.

2.5.2. Diffusion cells and receptor fluid

Franz-type glass diffusion cells (Laboratoires VERRE LABOMULA, Corbas, France) had 2-mL and 4-mL donor and receptor compartments, respectively. The membrane area available for

Table 1
Cristallite size, Lattice parameter and specific surface of CeO_2 and Ca^{2+}-doped CeO_2.

Compound	Cristallite size (nm)	Lattice parameter (nm)	Specific surface (m^2/g)
CeO_2	10.60	0.5410	10.66
15% Ca^{2+}-doped CeO_2	6.17	0.5414	26.82

Table 2
Efficacy of formulation.

Compound	n	J_{max} (%Q_0/h)	λ (min)	$E = \lambda/J_{max}$	%Q_0 (end of exposure)
Silicone membrane	9	0.30 ± 0.05	45 ± 28	1[a]	1.37 ± 0.22
H21 base	6	0.18 ± 0.02	45 ± 16	1.7[a]	0.98 ± 0.09
H21 CeO_2	6	0.13 ± 0.03*	70 ± 7	4.0[b]	0.53 ± 0.15*
H21CeO_2–Ca^{2+}	6	0.10 ± 0.02*	72 ± 23	5.1[b]	0.42 ± 0.06*
HASE-F polymer	4	0.12 ± 0.04*	106 ± 52	6.2[b]	0.61 ± 0.11*
HASE-F/Ce polymer	6	0.08 ± 0.05*	86 ± 12	10.7[c]	0.28 ± 0.26*

Superscript lower case letters show significant differences between each groups (a, b, c) ($p < 0.05$).
* Show significant difference with unprotected control (silicone membrane) (p-value < 0.05).

diffusion was 1.13 cm^2. Hank's Buffer Saline Solution (HBSS) was used as receptor fluid. The receptor compartments of the diffusion cells were immersed in a water bath setting at 36 °C to get a membrane surface temperature of 32 ± 1 °C on a magnetic stirrer bed. They contained a magnetic stir bar that allowed continuous mixing of the receptor fluid.

2.5.3. Application of formulations

Twenty minutes prior to POX exposure, 5.0 ± 0.3 mg/cm^2 of emulsions or polymers were applied on the membrane surface as homogenously as possible with a gloved finger.

2.5.4. Dosing

POX was loaded on the middle of the membranes as a liquid droplet (5 mg/cm^2, i.e. 4.9 μl) by using a positive displacement pipette (Microman M10, Gilson). The exposure duration was 6 h.

2.5.5. Sampling

Four hundred microliters of receptor fluid (RF) were collected regularly from 1hour and 30 min to the end of the exposure duration. The replenishment of same volume of fresh receptor fluid was performed at each sampling time.

2.6. Quantification of POX

The concentration of POX in the receptor fluid samples was determined by using an enzymatic method already described [7,51]. A stock solution of POX (100 mM) was prepared by the dilution of neat POX in absolute ethanol and stored at −20 °C. When required it was diluted to yield standard solutions from 1 to 25 nM. Stock solution of horse butyrylcholinesterase (BChE) and butyrylthiocholine iodide (BTCh) were prepared respectively at 1 mg/mL and 25 mM in HBSS and stored at +4 °C. Immediately prior to use, the BChE stock solution was diluted 25-fold ("enzyme solution") and the BTCh stock solution was diluted 10-times ("substrate solution"). The enzyme control (100% activity) consisted of 980 μl of enzyme mixed to 20 μl HBSS (repetition of 3 different cuvettes). In each cuvette, 20 μL of appropriately diluted samples of unknown POX concentration or standards of known POX concentration were mixed with 980 μl of enzyme. Cuvettes were covered with a sealing tape then incubated for 2 h at room temperature. 100 μL of the substrate was then added to each cuvette and the change in absorbance with time was measured spectrophotometrically at 400 nm over 2 min. Standard curves were obtained by plotting the concentration of POX standards versus the logarithm of the percent of enzyme activity remaining in each set of standards. The concentrations of POX in samples were derived from the linear portion of the calibration curve. All spectrophotometric measurements of enzymatic reaction rates were performed at 30 °C using a UV/VIS spectrophotometer (LAMBDA 35, PerkinElmer).

2.7. Data analysis

The cumulative amount of POX, expressed as percent of the applied dose (%Q_0), was plotted against time. For each replicate, maximal flux (J_{max}) values were calculated from the slope of the graph determined after equilibrium was reached, i.e. when the POX penetration rate became constant and maximum. The intercept of this slope with the x-axis corresponds to the apparent lag time (λ).

2.8. Formulations efficacy

As described in previous works [6,7], we chose to evaluate the barrier efficacy of products against POX from the ratio $E = \%\lambda/\%J_{max}$ (% of control values). Ideally, membranes pre-treated with an effective TSP should delay (higher λ) and slow down (lower J_{max}) the permeation of targeted chemicals. Formulations with E values higher than 1 (i.e. delaying and/or slowing down the permeation of POX) could be potentially effective as TSP. Conversely, products with E values equal to or lower than 1 could be viewed as having no effect or enhancing the permeation of POX, respectively.

2.9. Statistical analysis

Multivariate analysis of variance with the Kruskal–Wallis post-hoc test followed by the Dunn test (two-tailed p-value) comparing unprotected silicone membranes (controls) with protected ones (emulsions or polymers) were performed at each time of the penetration kinetic and for the J_{max}, λ and E parameters. Moreover, one-way ANOVA tests followed by unilateral Dunnett tests were used to determine whether these values were significantly lower or higher than the control group. A p-value lower than 0.05 was considered significant. All values were presented as mean ± SD ($n = 6$). The statistical software was XLSTAT.

3. Results

Firstly, the effect of NP on the efficacy when introduced in emulsion (Fig. 4) or when grafted (Fig. 5) were studied. Secondly, the dispersion of CeO_2 NP in formula vs. in polymeric matrix were compared (Table 2). Due to their standard deviation all λ were considered similar to unprotected controls (Table 2).

3.1. Effectiveness of emulsions

The base emulsion (H21) did not show an effective protection (Fig. 4, Table 2). Emulsion containing pure CeO_2 NPs or Ca^{2+}-doped CeO_2 NPs showed the same significant decrease of POX penetration in comparison to unprotected control. Maximal fluxes were 42% (CeO_2) and 33% (CeO_2–Ca^{2+}) of the control (Table 2). Amount of POX recovered in the receptor fluid at the end of exposure were 2–3-times reduced (Fig. 4, Table 2). The efficacy of formulated CeO_2 and Ca^{2+}-doped CeO_2 NPs were confirmed by their E values being greater than 1 (respectively 4.0 and 5.1).

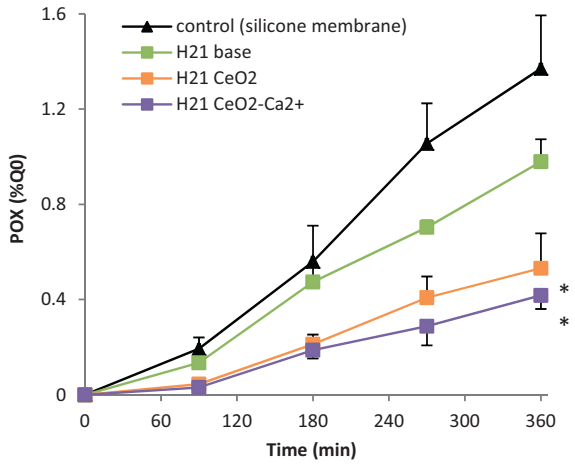

Fig. 4. Cumulative percent of the applied dose of POX penetrated through formulations (mean ± SD). Stars show significant differences in POX penetration (1 h 30 min–6 h) compared to the unprotected control (silicone membranes) (*$p < 0.005$).

3.2. Effectiveness of polymers

Both polymers showed a significant reduction of the maximal flux, from a 2-fold factor for HASE to 4-fold for CeO_2 NPs grafted to HASE polymer (Table 2). Penetrated percent of POX recovered in the receptor fluid at the end of exposure was 2–5-times reduced (Fig. 5, Table 2). The effectiveness of both polymers was confirmed by their E values significantly greater than 1 (Table 2). Moreover, the E value of HASE-F/CeO_2 polymer was significantly greater than the E value of HASE-F polymer (10.7 vs. 6.2) (Table 2, $p < 0.05$).

3.3. Comparative efficacy of the two dispersions ways of CeO_2 NPs

The comparison of CeO_2 NPs dispersed in emulsion or grafted to HASE-F polymer also provides information on how the grafting influences overall efficacy. E values show significant differences between formulated and grafted CeO_2 (4.0 vs. 10.7) (Table 2). Then the grafting positively impacts the efficiency of CeO_2 NPs.

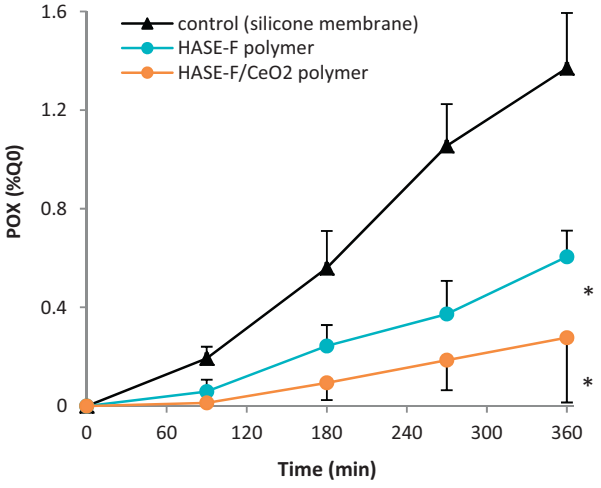

Fig. 5. Cumulative percent of the applied dose of POX penetrated through polymers (mean±SD). Stars show significant differences in POX penetration (1 h 30 min–6 h) compared to the unprotected control (silicone membranes) (*$p < 0.05$).

4. Discussion

To evaluate the efficacy against organophosphate POX we use in vitro permeation tests through silicone membranes as first screening tests. In this work, we study the best way to disperse and improve the protectant efficacy of cerium NPs. Firstly we measure the contribution of CeO_2 NPs on the protection efficiency. Secondly, since the doping of CeO_2 NP by calcium enhances the effectiveness for UV protection [32], we study its potential effect on the protection against OPs penetration by comparing effectiveness of pure and doped NPs dispersed in O/W emulsions. Finally, we study the influence of the two dispersion methods on the efficiency. Thereby, we compare the effectiveness of NPs dispersed in emulsion and once grafted to a new fluorocarbon HASE polymer.

4.1. Positive effect of CeO_2 NPs in formulations

The emulsion base (H21 base) is composed of 5% of PTFE, 5% of silicone and 10% of paraffin. These ingredients were chosen for their film-forming properties so as to create a barrier against the POX penetration. Moreover, perfluorinated polymers have a known effectiveness in TSP [16,52] due to their low surface tension energy giving them oleophobic and hydrophobic properties [53]. However, the H21 emulsion used as reference control does not show any efficiency. The ineffectiveness of the base emulsion can be explained: (1) silicone and paraffin are hydrophobic and lipophilic ingredients, they probably create affinity with the tested lipophilic agent POX and (2) the H21 base emulsion is composed with 5% of PTFE. Efficient perfluorinated-based TSP such as SERPACWA are composed with 100% perfluorinated compounds (50% of perfluoropolyether oil and 50% of PTFE) [52]. 5% of PTFE on the H21 base emulsion is not sufficient to provide an effective protection. The addition of the CeO_2 and calcium doped-CeO_2 NPs into H21 base emulsion (H21CeO_2 and H21CeO_2–Ca^{2+}) induces a significant effectiveness in comparison to unprotected controls ($E = 4.0–5.1$). Therefore, the efficiency of H21CeO_2 and H21CeO_2–Ca^{2+} emulsions in comparison to the H21 base demonstrates that the protection is due to the presence of NPs.

Perfluorinated HASE polymer (HASE-F) show an efficient protection against the penetration of POX ($E = 6.2$). The grafting of NPs onto polymer allows to disperse them easily in water thanks to the rheological properties of the HASE polymers that form physical gels in water at neutral pH. Thereby, neutralized suspension in water containing 10 wt.% of polymer or grafted polymer can be easily spread on silicone membrane. HASE-F/CeO_2 formulation shows a better efficiency in comparison to HASE-F ($E = 10.7$). Therefore, we demonstrate that (1) the application of fluorocarbon HASE polymer on silicone membrane reduces by half the permeation of POX, thanks to the repellent properties of the fluorinated polymer and (2) as well as for emulsions, the presence of CeO_2 NPs significantly reduces the permeation of POX as they are known to be active agents for their adsorption and degradation properties [11,22,25–27,34,54].

Moreover, Millerioux *et al.* [7] tested, with silicone membrane, the protective efficacy of O/W emulsion (BCw $E = 1.03$) and perfluorinated polymers-based cream (BC_p $E = 230$) against POX. Our emulsions and polymers containing NPs show a better protective efficiency than BCw due to the addition of NPs (E value respectively, 4.0 for H21CeO_2; 5.1 for H21CeO_2–Ca^{2+}; 6.2 for HASE-F and 10.7 for HASE-F/Ce). However, both NPs emulsions and polymers are less protective than BCp. BCp is a perfluorinated compounds-based barrier cream composed of 100% fluorinated compounds and difficult to spread, used here as a positive control. Therefore, the introduction of NPs in an emulsion or onto a thickener allows to create an efficient barrier against the penetration of POX that is less

expensive due to a lower amount of perfluorinated compounds and with better spreading properties.

4.2. Effect of the doping by calcium of CeO_2 NP for skin protection

Doping of CeO_2 NPs by calcium increase their UV filtration and makes its better to use for the solar skin protection [32]. It could be interesting to see if some similar properties could be observed for the skin protection against the penetration of OPs. The 15 mol.% of Ca^{2+} doping was chosen to reach the recommended dose to observed a gain in the efficiency of UV protection (>10%) [32]. H21CeO_2 and H21CeO_2–Ca^{2+} have the same protection efficiency (respectively, $E = 4.0$ and 5.1). The compared efficiency between both type of NPs introduced in emulsion does not highlight any enhanced efficiency of Ca^{2+}-doped CeO_2. Thus, the doping and the observed modifications of physicochemical properties are not sufficient to impact significantly the effectiveness of CeO_2 NPs in the case of OP skin protection.

The advantage of the emulsion formulation is to disperse active ingredients (NPs) in a matrix at lower cost and with good spreadability. Moreover, thanks to the presence of the ingredients, the coating is homogenous and film-forming that allows a good reproducibility of the results. Indeed, at the end of exposure, the relative standard deviation (RDS = SD/mean) of the percent of the initial dose (%Q_0) is nearly the same as unprotected control (16%): H21, 9%; H21CeO_2, 21%; H21CeO_2–Ca, 14%. But, due to their size and their high active surface NPs aggregate easily in aqueous solution making its difficult to realize homogeneous dispersions. Moreover, at the nano-state they can be an issue for safety assessments [35–40]. In that context, we propose a new approach to disperse NPs in formula: their covalent grafting onto HASE polymers that limit their toxicological impact on the environment [50].

4.3. Efficiency of CeO_2 NPs in emulsion or grafted to a thickening polymer

Since pure and calcium doped-CeO_2 NPs having the same protection, we choose to graft only the pure NPs. The advantages of the grafting are (1) to conserve the high active surface of NPs by better dispersing NPs and keeping them at the individual state [41] and (2) to limit the potential toxicological impact thanks to the covalent grafting of NP on a polymeric matrix [50]. The dispersion by grafting NPs to a thickening polymer ($E_{\text{HASE-F/CeO}_2} = 10.7$) show a better effectiveness than the dispersion in emulsion ($E_{\text{H21CeO}_2} = 4.0$). However, the deposit of the grafted polymer can slightly crack during the drying. Indeed, at the end of exposure, the relative standard deviation (RDS = SD/mean) of the percent of the initial dose (%Q_0) is 5-time higher for the HASE-F/CeO_2 (92%) than the HASE-F (18%, similar to unprotected membranes). The same ratio is observed for the $J_{\max}$ (39% for HASE-F/Ce polymer and 19% for the H21CeO_2 emulsion). Although the CeO_2 NPs grafted onto HASE-F polymer show a better effectiveness, the risk of a cracking increases appreciably the standard deviation of our results. Thus, the choice is a compromise between a good effectiveness or a film-forming spreading and a good reproducibility.

5. Conclusion

In this work, we demonstrated that relative to CeO_2 NPs, Ca^{2+}-doped CeO_2 NPs do not enhance efficiency for the skin protection against the penetration of OP toxic agent POX. We also studied two ways to integrate CeO_2 NPs in TSP: formulating them into O/W emulsions or grafting them on the fluorocarbon associative polymer (HASE-F). These two formulations were more effective in comparison to their base (H21 base and HASE-F polymer): the use of NPs enhances protection properties. This tendency must be verified by other in vitro tests using excised pig or human skin.

In conclusion, the emulsion formulation is the best way to obtain film-forming coating allowing a good reproducibility of the penetration results. However, the use of free NPs as an active ingredient has two main issues: they can easily aggregate in emulsion and they can induce a possible healthy risk since NP penetration and accumulation in biological membranes is suspected. On the contrary, the grafting of NPs on fluorinated polymeric matrix link them covalently to macromolecules that allows to disperse them homogeneously without any toxicological issues of the NPs. But, the deposit cracks at drying and thus the reproducibility is impacted. Therefore, the best way to disperse NPs could be to introduce the grafted polymer in a film-forming formula.

Conflict of interest

None declared.

Acknowledgment

The authors would like to acknowledge Direction Générale de l'Armement for their grant and support.

References

[1] J.K. Smart, History of Chemical and biological warfare: an american perspective. Medical Aspects of Chemical and Biological Warfare, in: F.R. Sidell, E.T. Takafuji, D.R. Franz (Eds.), From the Textbook of Military Medicine, 1997, Chapter 2.
[2] T. Okumura, K. Taki, K. Suzuki, T. Satoh, The Tokyo Subway Sarin Attack: Toxicological Whole Truth, in: C. Ramesh Gupta (Ed.), From the Handbook of Toxicology of Chemical Warfare Agents, 2009, Chapter 4.
[3] United Nations Mission to Investigate Allegations of the Use of Chemical Weapons in the Syrian Arab Republic Report on the Alleged Use of Chemical Weapons in the Ghouta Area of Damascus on 21 August 2013.
[4] K. Musilek, M. Dolezal, F. Gunn-Moore, K. Kuca, Design, evaluation and structure—activity relationship studies of the AChE reactivators against organophosphorus pesticides, Med. Res. Rev. 31 (2011) 548–575.
[5] A. Watson, D. Opresko, R. Young, V. Hauschild, J. King, K. Bakshi, et al., Organophosphate Nerve Agents, in: C. Ramesh Gupta (Ed.), From the Handbook of Toxicology of Chemical Warfare Agents, 2009, Chapter 6.
[6] J. Millerioux, C. Cruz, A. Bazire, G. Lallement, L. Lefeuvre, D. Josse, In vitro selection and efficacy of topical skin protectants against the nerve agent VX, Toxicol. In Vitro 23 (April) (2009) 539–545.
[7] J. Millerioux, C. Cruz, A. Bazire, V. Polly, G. Lallement, L. Lefeuvre, et al., Evaluation of in vitro tests to assess the efficacy of formulations as topical skin protectants against organophosphorus compounds, Toxicol. In Vitro 23 (February) (2009) 127–133.
[8] V. Vallet, C. Cruz, J. Licausi, A. Bazire, G. Lallement, I. Boudry, Percutaneous penetration and distribution of VX using in vitro pig or human excised skin validation of demeton-S-methyl as adequate simulant for VX skin permeation investigations, Toxicology 246 (April (3)) (2008) 73–82.
[9] F.K. Chang, M.L. Chen, S.F. Cheng, T.S. Shih, I.F. Mao, Field protection effectiveness of chemical protective suits and gloves evaluated by biomonitoring, Occup. Environ. Med. 64 (November) (2007) 759–762.
[10] D.H. Brouwer, R.J. Aitken, R. Oppl, J.W. Cherrie, Concepts of skin protection: considerations for the evaluation and terminology of the performance of skin protective equipment, J. Occup. Environ. Hyg. 2 (2005) 425–434.
[11] O. Koper, K.J. Klabunde, Reactive nanoparticles as destructive adsorbents for biological and chemical contamination, US Patent WO 01/78506 A1, 2001.
[12] E.H. Braue, S.T. Hobson, J. White, R. Bley, Actives topical skin protectants using polyoxometallates, US Patent 6,420,434 B1, 2002.
[13] S.T. Hobson, E.H. Braue, E.K. Lehnert, K.J. Klabunde, O.P. Koper, S. Decker, Active topical skin protectants using reactive nanoparticles, US Patent 6,403,653 B1, 2002.
[14] E.H. Braue, M.M. Mershon, C.R. Braue, R.A. Way, Active topical skin protectants containg S-330, US Patent 6,472,438 B1 2002.
[15] S.T. Hobson, E.H. Braue, E.K. Lehnert, K.J. Klabunde, S. Decker, C.L. Hill, et al., Active topical skin protectants using combinations of reactive nanoparticles and polyoxometalates or metal salts, US Patent 6,410,603 B1 2002.
[16] R.P. Chilcott, C.H. Dalton, I. Hill, C.M. Davison, K.L. Blohm, E.D. Clarkson, et al., Evaluation of a barrier cream against the chemical warfare agent VX using the domestic white pig, Basic Clin. Pharmacol. Toxicol. 97 (July) (2005) 35–38.
[17] S.T. Lin, K.J. Klabunde, Adsorption and decomposition of phosphorus compounds, Langmuir 1 (1985) 600–605.
[18] Y.-X. Li, O. Koper, M. Atteya, K.J. Klabunde, Adsorption and decomposition of organophosphorus compounds on nanoscale metal oxide particles. In situ

GC–MS studies of pulsed microreactions over magnesium oxide, Chem. Mater. 4 (1992) 323–330.
[19] S. Sundarrajan, S. Ramakrishna, Fabrication of nanocomposite membranes from nanofibers and nanoparticles for protection against chemical warfare stimulants, J. Mater. Sci. 42 (2007) 8400–8407.
[20] A. Saxena, A.K. Srivastava, B. Singh, A.K. Gupta, M.V.S. Suryanarayana, P. Pandey, Kinetics of adsorptive removal of DECIP and GB on impregnated Al_2O_3 nanoparticles, J. Hazard. Mater. 175 (2010) 795–801.
[21] G.W. Wagner, L.R. Procell, R.J. O'Connor, S. Munavalli, C.L. Carnes, P.N. Kapoor, et al., Reactions of VX, GB, GD, and HD with nanosize Al_2O_3. Formation of aluminophosphonates, Am. Chem. Soc. 123 (2001) 1636–1644.
[22] A. Saxena, A.K. Srivastava, B. Singh, A. Goyal, Removal of sulphur mustard, sarin and simulants on impregnated silica nanoparticles, J. Hazard. Mater. 211–212 (2012) 226–232.
[23] B. Cojocaru, V.I. Parvulescu, E. Preda, G. Iepure, V. Somoghi, E. Carbonell, et al., Sensitizers on inorganic carriers for decomposition of the chemical warfare agent yperite, Environ. Sci. Technol. 42 (2008) 4908–4913.
[24] Y.-X. Li, K.J. Klabunde, Nano-scale metal oxide particles as chemical reagents. Destructive adsorption of a chemical agent simulant, dimethyl methylphosphonate, on heat-treated magnesium oxide, Langmuir 7 (1991) 1388–1393.
[25] G.W. Wagner, P.W. Bartram, O. Koper, K.J. Klabunde, Reactions of VX, GD, and HD with nanosize MgO, J. Phys. Chem. B 103 (April) (1999) 3225–3228.
[26] G.W. Wagner, O. Koper, E. Lucas, S. Decker, K.J. Klabunde, Reactions of VX, GD, and HD with Nanosize CaO: Autocatalytic Dehydrohalogenation of HD, J. Phys. Chem. B. 104 (June) (2000) 5118–5123.
[27] B. Singh, A. Saxena, A.K. Nigam, K. Ganesan, P. Pandey, Impregnated silica nanoparticles for the reactive removal of sulphur mustard from solutions, J. Hazard. Mater. 161 (January (30)) (2009) 933–940.
[28] A. Corma, P. Atienzar, H. García, J.-Y. Chane-Ching, Hierarchically mesostructured doped CeO_2 with potential for solar-cell use, Nat. Mater. 3 (2004) 394–397.
[29] L. Vivier, D. Duprez, Ceria-based solid catalysts in organic chemistry, ChemSusChem 3 (2010) 654–678.
[30] S. Tsunekawa, T. Fukuda, A. Kasuya, Blue shift in ultraviolet absorption spectra of monodispersex nanoparticles, J. Appl. Phys. 87 (2000) 1318–1321.
[31] S. Tsunekawa, J.-T. Wang, Y. Kawazoe, A. Kasuya, Blueshifts in the ultraviolet absorption spectra of cerium oxide nanocrystallites, J. Appl. Phys. 92 (2003) 3654–3656.
[32] L. Truffault, T. Ma, T. Devers, K. Konstantinov, V. Harel, C. Simmonard, et al., Application of nanostructured Ca doped CeO_2 for ultraviolet filtration, Mater. Res. Bull. 45 (2010) 527–535.
[33] M.H. Kuchma, C.B. Komanski, J. Colon, A. Teblum, A.E. Masunov, B. Alvarado, et al., Phosphate ester hydrolysis of biologically relevant molecules by cerium oxide nanoparticles, Nanomed.: Nanotechnol. Biol. Med. 6 (2010) 738–744.
[34] N.M. Zholobak, V.K. Ivanov, A.B. Shcherbakov, A.S. Shaporev, O.S. Polezhaeva, A.Y. Baranchikov, et al., UV-shielding property, photocatalytic activity and photocytotoxicity of ceria colloid solutions, J. Photochem. Photobiol. B 102 (January (10)) (2011) 32–38.
[35] S. Hackenberg, A. Scherzed, A. Technau, M. Kessler, K. Froelich, C. Ginzkey, et al., Cytotoxic, genotoxic and pro-inflammatory effects of zinc oxide nanoparticles in human nasal mucosa cells in vitro, Toxicol. In Vitro 25 (April) (2011) 657–663.
[36] R.K. Shukla, V. Sharma, A.K. Pandey, S. Singh, S. Sultana, A. Dhawan, ROS-mediated genotoxicity induced by titanium dioxide nanoparticles in human epidermal cells, Toxicol. In Vitro 25 (February) (2011) 231–241.
[37] B.C. Heng, X. Zhao, S. Xiong, K.W. Ng, F.-Y.-C. Boey, J.S.-C. Loo, Cytotoxicity of zinc oxide (ZnO) nanoparticles is influenced by cell density and culture format, Arch. Toxicol. 85 (June) (2011) 695–704.
[38] F. Dechsakulthorn, A. Hayes, S. Bakand, L. Joeng, C. Winder, In vitro cytotoxicity assessment of selected nanoparticles using human skin fibroblasts, AATEX (2008) 397–400.
[39] T. Boutard, B. Rousseau, C. Couteau, C. Tomasoni, C. Simonnard, C. Jacquot, et al., Comparison of photoprotection efficiency and antiproliferative activity of ZnO commercial sunscreens and CeO_2, Mater Lett. 108 (October) (2013) 13–16.
[40] I. Celardo, M. De Nicola, C. Mandoli, J.Z. Pedersen, E. Traversa, L. Ghibelli, Ce^{3+} ions determine redox-dependent anti-apoptotic effect of cerium oxide nanoparticles, ACS Nano 5 (June (28)) (2011) 4537–4549.
[41] A. Zenerino, S. Amigoni, E. Taffin de Givenchy, D. Josse, F. Guittard, New fluorinated hybrid organic/inorganic water soluble polymeric network, Polymer 54 (October) (2013) 6089–6095.
[42 S. Dai, K.C. Tam, R.D. Jenkins, Light Scattering of hydrophobically modified alkali-soluble emulsion (HASE) polymer: ionic strength and temperature effects, Macromol. Chem. Phys. 202 (January (1)) (2001) 335–342.
[43] K. Nagashima, V. Strashko, P.M. Macdonald, R.D. Jenkins, D.R. Bassett, Diffusion of model hydrophobic alkali-swellable emulsion associative thickeners, Macromolecules 33 (December) (2000) 9329–9339.
[44] W. Ng, K. Tam, R. Jenkins, Rheological properties of methacrylic acid/ethyl acrylate co-polymer: comparison between an unmodified and hydrophobically modified system, Polymer 42 (January) (2001) 249–259.
[45] F. Petit, I. Iliopoulos, R. Audebert, S. Szönyi, Associating polyelectrolytes with perfluoroalkyl side chains: aggregation in aqueous solution, association with surfactants, and comparison with hydrogenated analogues, Langmuir 13 (August) (1997) 4229–4233.
[46] Y. Li, P. Li, J. Wang, Y. Wang, H. Yan, C. Dong, et al., Thermodynamics of micellization for partially fluorinated cationic gemini surfactants and related single-chain surfactants in aqueous solution, J Colloid Interface Sci. 287 (July (1)) (2005) 333–337.
[47] R. Oda, I. Huc, D. Danino, Y. Talmon, Aggregation properties and mixing behavior of hydrocarbon, fluorocarbon, and hybrid hydrocarbon-fluorocarbon cationic dimeric surfactants, Langmuir 16 (December) (2000) 9759–9769.
[48] M. Pabon, J.M. Corpart, Fluorinated surfactants: synthesis, properties, effluent treatment, J. Fluorine Chem. 114 (April) (2002) 149–156.
[49] O. Oddes, S. Amigoni, E. Taffin de Givenchy, P. Reeve, Y. Duccini, F. Guittard, Influence of fluorinated segments of variable length on the thickening properties of a model HASE skeleton, J. Appl. Polym. Sci. 120 (June (5)) (2011) 2685–2692.
[50] L. Clément, A. Zenerino, C. Hurel, S. Amigoni, E. Taffin de Givenchy, F. Guittard, et al., Toxicity assessment of silica nanoparticles, functionalised silica nanoparticles, and HASE-grafted silica nanoparticles, Sci. Total Environ. 450–451 (April (15)) (2013) 120–128.
[51] W.K. Loke, B. Karlsson, L. Waara, A.G. Nyberg, G.E. Cassel, Enzyme-based microassay for accurate determination of soman in blood samples, Anal. Biochem. 257 (March (1)) (1998) 12–19.
[52] M.J. McCrerry, Topical skin protectant, US Patent 5,607,979, 1997.
[53] A. Zenerino, T. Darmanin, E. Taffin de Givenchy, S. Amigoni, F. Guittard, Connector ability to design superhydrophobic and oleophobic surfaces from conducting polymers, Langmuir 26 (August (17)) (2010) 13545–13549.
[54] S. Yabe, Cerium oxide for sunscreen cosmetics, J. Solid State Chem. 171 (March (1)) (2003) 7–11.